Studies on Some Inorganic Oxide Glasses Used as Gamma-Ray Shields and for Radio-Active Waste Encapsulation

A.M. Abdel-Ghany [1], M.S.S. Saad [1], I.I. Bashter [2], T.Z. Amer [3], S.M. Salem [4] and A.G. Mostafa [4]*

[1.] Basic Science Dept., Faculty of Engineering Science, Sinai Univ., El-Arish, Egypt
[2.] Phys. Dept., Faculty of Science, Zagazig Univ., Zagazig, Egypt
[3.] Phys. Dept., Faculty of Science, Al-Azhar Univ., Women Branch, Nasr City, Cairo, Egypt
[4.] Phys. Dept., Faculty of Science, Al-Azhar Univ., Nasr City, Cairo, Egypt
*drahmedgamal@yahoo.com

Abstract: Tungsten-doped sodium-phosphate glasses with varying tungsten contents [0, 5, 10, 15 and 20 mol %] have been prepared, where all samples appeared transparent. Infrared absorption measurements were carried out to identify the structural building groups in their networks where it showed approximate stability of the glass network former to glass network modifier ratio. It was found that, as WO_3 was gradually increased, the density increased while the molar volume decreased. These samples showed also shielding behavior towards the effects of gamma ray radiation, and the total gamma-ray mass attenuation coefficient increased and the half value layer decreased, with the increase of WO_3. The sample containing 20 mol% WO_3 represents the suitable one for low energy gamma-ray (especially for 332 keV). The temperature dependence of both conductivity and exponent factor (s) are well interpreted applying the correlated barrier hopping (CBH) model. The obtained conductivity data showed that all samples behave like semi-conductors. The conductivity as well as the dielectric constant and loss factor showed an increase, at low WO_3 content, while they showed a gradual decrease at high WO_3 content.
[Abdel-Ghany AM, Saad MMS, Bashter II, Amer TZ, Salem SM and Mostafa AG. **Studies on Some Inorganic Oxide Glasses Used as Gamma-Ray Shields and for Radio-Active Waste Encapsulation.** *Nat Sci* 2014;12(12):162-170]. (ISSN: 1545-0740). http://www.sciencepub.net/nature. 22

Keywords: Oxide Glasses; Infrared Spectroscopy; Gamma Ray Shielding; Density and Molar Volume; Conductivity and Dielectric Constant

1. Introduction

Nowadays, the universal uses of many radio-active sources in approximately all daily life fields make the mankind life dangerous. These sources after sometimes will leave many radio-active wastes, which are also of high dangerous effect upon all the existing creations. Therefore, the search for shielding materials is a matter of interest – specially - for users. In the same time, the leaved radio-active wastes must be delivered in a safe way in order to feel safe environment. Although, many articles have been published concerning with this problem, more research work are still needed. Reise et al, have investigated some lead-iron phosphate glasses in order to immobilize high-level radio-active wastes [1]. Karabulut et al, have investigated some iron-phosphate glasses containing high level nuclear waste components (as UO_2, Cs_2O and Bi_2O_3) for nuclear waste encapsulation [2]. Shih and Chin have studied some lead-phosphate glasses incorporated with mixed metal oxides, and the glass batches were melted with radio-nuclide wastes. They found that the dissolution rate of the nuclide wastes decreased as the mixed metallic cations were increased [3]. It was found also that, gamma-ray mass attenuation coefficient increased gradually as barium cations was increased in different phosphate glasses [4].

On the other hand, the electrical properties of a material that can be used as gamma-ray shield must be also examined. The continuous studies on electric and dielectric properties of such like glasses help not only to have a comprehensive idea about the ac conduction mechanism but also to give some additional information about the structural aspects as well as the micro-electronic device technology. The work along these lines has been carried out in recent years on a variety of inorganic glass systems where it yields valuable information [5, 6]. The ac conductivity of tungsten phosphate [7] and iron phosphate glasses [8] and also the dielectric dispersion of vanadium telluride [9] and molybdenum phosphate glasses [10] have been studied and the results have been interpreted in terms of different models such as quantum mechanical tunneling (QMT) and hopping over barrier (HOB).

However, in this article, a trial will be done to prepare some sodium-phosphate glasses containing tungsten tri-oxide. The properties of the prepared glasses will be thoroughly studied aiming to obtain materials, can be used as a good shield from harmful rays and /or for radio-active waste encapsulation.

2. Experimental work

Glasses having the composition [30 mol% Na_2O - (70-x) mol% P_2O_5 - x mol% WO_3], (x=0, 5, 10, 15 and 20 mol %), have been prepared by the conventional melt quenching method. Batches, to produce 20 g of each glass sample, were ground and mixed well, and were then placed in porcelain crucibles and heated gradually from room temperature up to 1200°C to expel water and ammonia gradually. The melts were left at 1200°C for 2h, and they were stirred several times in order to obtain homogenous glasses. Then they were quenched in air, and just, after sitting, the solid glasses were directly transferred to the annealing furnace at 250°C and the furnace was turned off and was left to cool to room temperature over night with a rate of cooling equals about 0.5 K/min.

The visual examination of the prepared samples showed that all the obtained solid samples are transparent, and exhibit an amorphous nature and short-range order character. Also, they are found free from visible in-homogeneities, such as inclusions, cracks or air bubbles [11].

Infrared absorption spectra of the studied glasses were recorded at room temperature in the wave number range of (400-4400 cm^{-1}), using Fourier- transform infrared (FTIR) Berken Elmer spectrometer; model RTX. The KBr disk technique was used where about 3mg of the powder sample was mixing well with about 200 mg KBr and then pressed to obtain disks suitable for IR measurements.

Density measurements were carried out applying Archimedes principle whereas the samples were weighted in both air and toluene as an immersion liquid of stable density (d= 0.8655 g/cm^3 at RT) using an electric balance with 4-decimal digits. The molar volume values were then calculated using the experimentally obtained density values. The empirical values of both density and molar volume were also calculated for comparison.

The values of the total mass attenuation coefficients $[(\mu/\rho)_{m(total)}]$ of the studied glasses were calculated applying Win X-COM program, based on the mixture rule , using equation (1) [12],

$$\left(\frac{\mu}{\rho}\right)_{m(total)} = \sum_{i=0}^{n} w_i \left(\frac{\mu}{\rho}\right)_{m(i)} \quad \text{.....(1)}$$

Where w_i is the fractional weight of the oxides in a glass sample, and $(\mu/\rho)_{m(i)}$ is the mass attenuation coefficient of such component.

The half value layers (HVL) of the studied glasses were also calculated according to equation (2), [12],

$$HVL = 0.693 / \mu \quad \text{.....(2)}$$

For the electrical conductivity measurements, the solid glasses were polished to obtained disk shape samples with 8 mm diameter and 1 mm thickness. The samples were cleaned and sandwiched between two electrodes of silver paste to obtain good electrical contact. The measurements were performed using LRC Bridge (model SR 270) at three different fixed frequencies [1, 10, and 100 kHz] and in the temperature range (from 300 to 460).

3. Results and Discussion

It is suitable firstly to obtain a complete idea about the internal structural groups in the glass network. Therefore infrared analysis was applied here and the obtained IR spectra in the range from 400 to 4000 cm^{-1} at RT, are exhibited in Fig. (1).

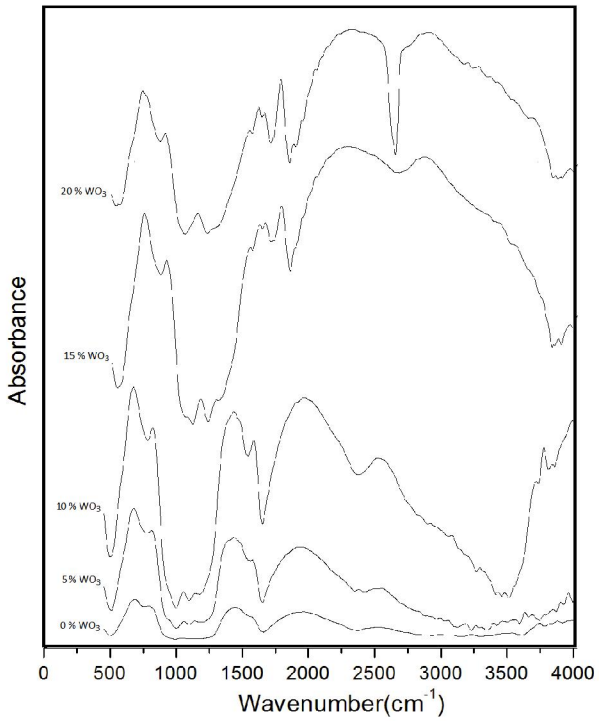

Figure 1. The obtained IR absorption spectra

It is known that all bands appeared approximately in the range from 2200 to 4000 cm^{-1} can be attributed to H_2O vibration, while the bands appeared around 1600 cm^{-1} can be attributed to the stretching vibration of H-O bond [13]. That is, the range of interest is only between 400 and 1600 cm^{-1} for the studied glasses. The appearance of some bands beyond 2000 cm^{-1} and that one appeared around 1600 cm^{-1} can be taken as evidence for the

presence of some –OH and H-O-H groups which may be due the used KBr disk technique [13].

Accordingly, the range from 400 to 1600 cm^{-1} was thoroughly examined by applying the de-convolution program to extract as really as possible the correct IR bands. Fig. (2), shows the de-convoluted spectrum of the sample contains 10 mol% WO_3 as a representative figure.

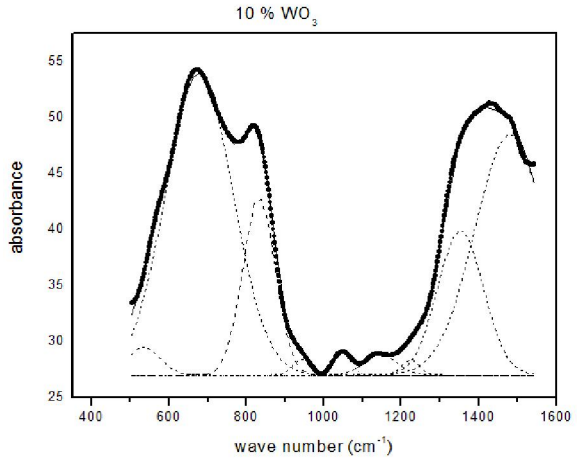

Figure 2. The de-convoluted spectrum of sample that contains 10 mol% WO_3, as a representative figure

The obtained de-convoluted IR bands appeared in the spectra of the studied glasses are listed in Table (1).

Table 1. The characteristic frequencies obtained from the de-convoluted IR spectra

Number of peaks	0% WO_3	5% WO_3	10% WO_3	15% WO_3	20% WO_3
1	1442	1429	1430	1440	1441
2	1222	1241	1236	1248	1232
3	1139	1135	1136	1166	1123
4	1038	1054	1049	1095	1034
5	939	944	936	941	940
6	789	812	819	820	816
7	680	675	673	669	661
8	590	577	575	594	586
9	475	478	486	490	494

Inspecting these bands, it can be concluded that:

1. The band appeared around 1440 cm^{-1}, can be assigned to the stretching vibration of phosphorous-oxygen double bond of the form (P=O) [14].
2. The band that appeared between 1222 and 1248 cm^{-1} can be assigned to the asymmetric stretching vibration of O-P-O, [15] and/or the stretching vibration of phosphorous-oxygen double bond (P=O) [14].
3. The band that appeared around 1150 cm^{-1} can be assigned to the stretching vibration of $P\text{-}O^-$ (non-bridging oxygen bond) [16]
4. At about 1040 cm^{-1}, there appeared a band which can be attributed to the stretching vibration of P-O-P bond [17, 18].
5. The frequency band that appeared in the range from 939 to 944 cm^{-1} may be due to P-O-P [19, 20].
6. The band which appeared between 789 and 816 cm^{-1} may be due to P–O–P symmetric stretching vibration [20].
7. The band appeared at 670 cm^{-1} is attributed to the P-O-P symmetric stretching vibration [14]
8. The band appeared in the range from 575 to 594 cm^{-1} may be assigned to O=P-O bending vibration [14].
9. The band that appeared in the range from 494 to 475 cm^{-1} can be assigned to the bending vibration of O-P-O units [21-22], and /or due to WO_4 groups [22].

According to the IR results, it can be stated that, phosphorous represents the major glass network former (GNF) cations while sodium represents the major glass network modifier (GNF) cations. It is observed also that, the approximate stability of the band positions in all glasses may indicated that tungsten replaces phosphorous to act only as GNF, and this mains that the ratio GNF to GNM is stable as well as the number of the non-bridging oxygen. It can be stated also that, the observed higher wave number of (P–O–P) stretching arises from the smaller P–O–P bond angle owing to the higher field strength and the small size of sodium cations, which results in shortening the chain length of phosphate glasses due to the de-polymerization of the glass network structure [23].

The presence of more than one frequency assigned the P–O–P stretching vibration mode, was attributed previously by Donna [24] to different molecular environments that arise from differences in phosphate tetrahedral chain length inside the glass network, and/or the presence of different species of tetrahedral units with different number of non-bridging oxygen anions.

After obtaining such idea about the internal structure of the studied glasses and in order to study the total gamma ray mass attenuation coefficient, the density values must be firstly obtained.

Although, density of solids is mostly the simplest physical property that can be measured, it is highly informative property if the structure of a material has to consider [25]. However, the experimental density (ρ^{exp}) values of the studied glass samples was measured using Archimedes principle applying equation (3),

$$\rho_{exp} = \frac{M_a}{M_a - M_t} \rho_t \quad (3)$$

Where: M_a and M_t are the masses of the sample in air and toluene respectively and ρ_t is the density of toluene.

Fig. (3), shows the change in the experimental density values as a function of WO_3 content. The empirical densities (ρ_{emp}) were also calculated applying equation (4) and were exhibited in the same figure for comparison.

$$\rho_{emp} = \sum_j \rho_j \cdot p_j \quad (4)$$

where $\rho_1, \rho_2, \rho_3, \ldots \rho_j$ are the densities of the constituting oxides and $P_1, P_2, P_3, \ldots\ldots\ldots, P_j$ are the percentage weights of the oxides composing such glass sample.

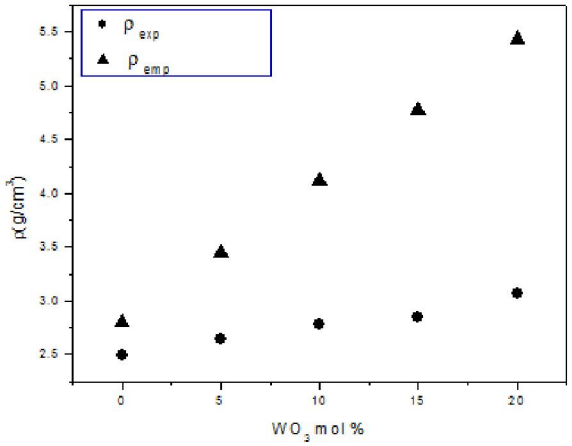

Figure 3. The change in the experimental and empirical densities versus WO_3 content

From this figure, it is seen that as WO_3 content was gradually increased from zero up to 20 mol%, both the experimental and the empirical densities increased gradually and linearly from 2.49 up to 3.07 g/cm^3, and from 2.79 to 5.44 g/cm^3, respectively. The rate of increase is 0.029 g/cm^3 mol, for the experimental values and it is 0.116 g/cm^3 mol, for the empirical ones. Such increase appeared to be logic, since the atomic weight of tungsten (183.84 g/mol) is much larger than that of phosphorus (30.97 g/mol).

It is of interest to calculate the molar volume values, since it relates directly to the internal spatial structure of materials. However, both the experimental and the empirical molar volume values were calculated using equation (5 and 6) respectively,

$$(V_m)_{exp} = (M_i / \quad _{exp}) \quad (5)$$
$$(V_m)_{emp} = (M_i / \quad _{emp}) \quad (6)$$

Fig. (4), represents the variation of both the experimental and the empirical molar volume values of the studied glasses as a function of WO_3 content.

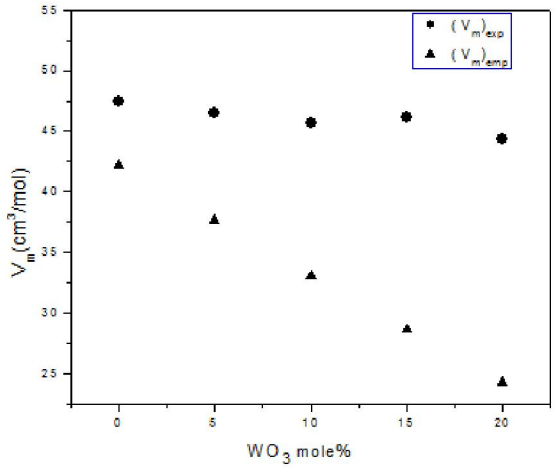

Figure 4. The change of the experimental and empirical molar volume versus WO_3 content

It can be seen that both the experimental and the empirical molar volume values decreased gradually from 47.39 to 44.37 cm^3/mol and from 42.17 to 24.99 cm^3/mol respectively, with the gradual replacement of P_2O_5 by WO_3. The rate of such decrease is 0.155 and 0.604 cm^3/mol respectively. Such decrease may be due to the following reasons:

A) The gradual decrease in the number of oxygen anions in the glass network, since five oxygen anions are replaced only by threes.

B) The gradual decrease of the positive cations also, since two phosphorous cations are replaced by only a single tungsten cation.

C) The differences between the covalent radii of both phosphorus (1.06A^o) and tungsten (1.3A^o) (where two phosphorus is approximately of (2.12A^o)).

All these factors act to reduce the volume occupied by one mole of these glasses as WO_3 was gradually increased.

It was stated previously, in the experimental section, that the visual examination of the prepared samples indicated that all samples exhibit an amorphous nature and they appeared also transparent. These observations, are now confirmed when expecting the observed large difference between both the experimental and the empirical density and molar volume values – specially – at high tungsten oxide content.

From another point of view, the universal uses of many types of radio-active sources are of

dangerous effect, especially for users, since they have to be approximately in continuous contact to different harmful rays. Accordingly, it is possible to check the shielding properties of the prepared glass samples for low and high γ-ray energies, and to calculate their gamma ray mass attenuation coefficient as well as the corresponding half value layers (HVL). That is these glasses were checked to conclude whether they can be used as transparent shield for gamma-ray or not?

The γ-ray total mass attenuation coefficients $[(\mu/\rho)_{m(total)}]$ have been calculated using Win X-COM program,

1. Firstly at different low γ-ray energies (332, 663, 1173 and 1332 KeV), emitted from ^{180}Hf, ^{137}Cs and ^{60}Co (for both 1173 and 1332) respectively [12]. Fig. (5) shows the change in the total γ-ray mass attenuation coefficient with the gradual increase of tungsten oxide where a gradual increase of $(\mu/\rho)_{m(total)}$, can be easily observed.

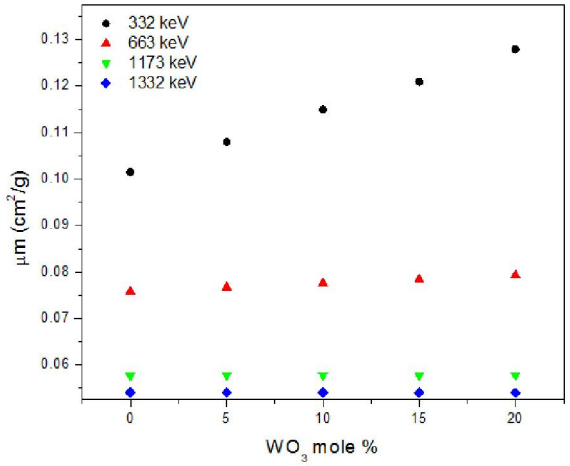

Figure 5. The mass attenuation coefficient versus WO_3 content for different low γ-ray energies

2. Secondly, Fig. (6) shows the change in the mass attenuation coefficient of the studied glasses at high γ-ray energies (10, 20, 30, 70 and 100 MeV). It appeared that as tungsten oxide was gradually increased, the mass attenuation coefficient increased.

The HVL of the studied glasses was also calculated for the same γ-ray energies considered above. The obtained values as a function of tungsten oxide are represented in Figs (7 & 8) for the low and high energy γ-rays respectively. It can be seen obviously that the HVL decreased gradually with the gradual increase of tungsten oxide content.

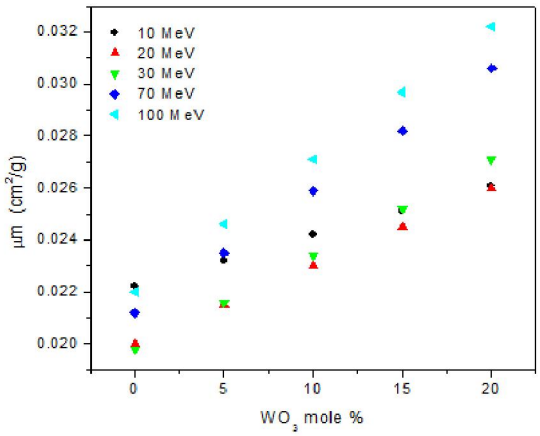

Figure 6. The mass attenuation coefficient as function of WO_3 content for different high γ-ray energies

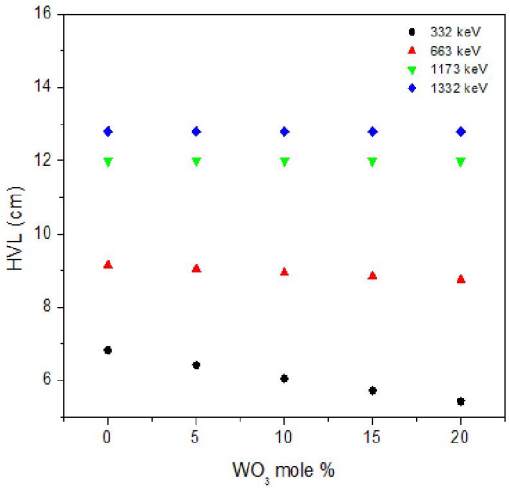

Figure 7. The HVL of the investigated glasses versus WO_3 content for different low γ-ray energies

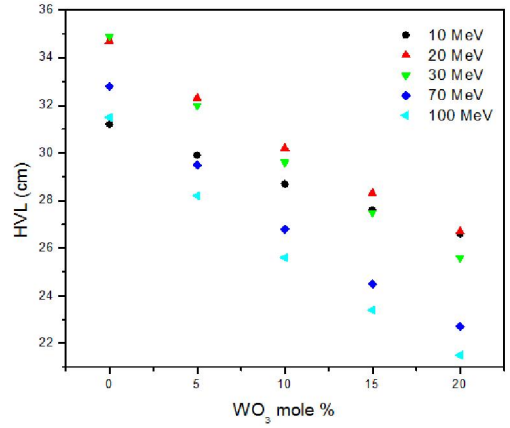

Figure 8. The HVL of the investigated glasses versus WO_3 content for different high γ-ray energies

The observed increase in the γ-ray mass attenuation coefficient as well as the corresponding

decrease in the HVL of the studied glasses can be attributed to the gradual replacement of P_2O_5 by WO_3. This can be understood logically by knowing that the γ-ray mass attenuation coefficient of tungsten oxide is higher than that of phosphorus oxide and the HVL of tungsten oxide is smaller than that of phosphorus oxide. The μ (cm^2/g) and HVL (cm) for WO_3 and P_2O_5 are exhibited in Table (2) for comparison [12].

Table 2. μ (cm^2/g) and HVL (cm) for phosphorus and tungsten oxides at different low γ-ray energies [12]

E(KeV)	μ (cm^2/g)		HVL(cm)	
	WO_3	P_2O_5	WO_3	$P2O_5$
332	0.0849	0.02538	8.163	27.305
662	0.08868	0.02653	7.815	26.121
1173	0.09073	0.02719	7.638	25.487
1332	0.09107	0.02731	7.610	25.375

Generally, it can be stated that, all the studied glasses can be used as gamma-ray shield and to capsulate nuclear radio-active wastes before interment underground. These samples work well for law than for high gamma-ray energies. It is worth to state also that the sample containing 20 mol% WO_3 appeared to be of high suitability to act as shield for the 332 keV gamma-ray energy, since it presents the highest μ_t coefficient and the lowest HVL values.

From another point of view, it is known that when gamma-ray falls on a material, some electric charges may induce and accumulated on such material which forms an effective dangerous charge. If such glass may be used as a shield, it has to posses semiconducting properties. Therefore, the electrical transport properties of the prepared glasses were checked in order to be sure that these glasses must behave like semi-conductors and the formed charges can be drown to the earth through a contact earthy cable.

The total conductivity [$\sigma_T(\omega) = \sigma_{dc} + \sigma_{ac}$] has been measured as a function of temperature and frequency, and Fig. (9) shows the total conductivity temperature dependence at different fixed frequencies, for the sample that contains 15 mol % WO_3, as a representative curve, and all other samples showed similar behavior.

All the studied glasses showed that the total conductivity (σ_t (ω)) increased with the increase of temperature, which reveals that all samples behave like semiconductors. It is seen that the change in $\ln(\sigma_t)$ is entirely temperature and frequency dependent in the used temperature range.

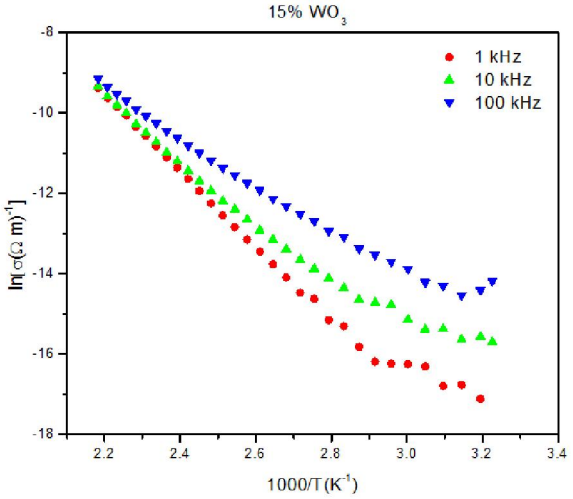

Figure 9. Total conductivity temperature dependence at three frequencies for the sample containing 15 % WO_3, as representative figure

It is known also that, the ac conductivity of all amorphous materials and glasses follows the universal power law,

$$\sigma(\omega) = A\,\omega^s \qquad (4)$$

Where A is a constant (weakly temperature dependent), ω is the angular frequency and **s** is the exponent factor, where the change of **s** with temperature gives accurately the conduction mechanism in an amorphous solid [20].

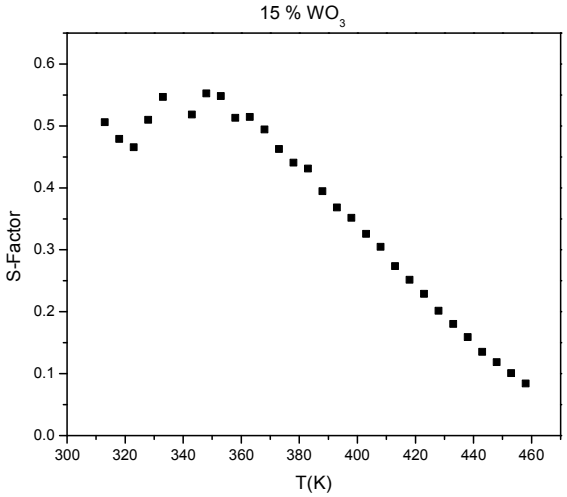

Figure 10. The variation of S-factor versus temperature for the sample containing 15 mol% WO_3, as representative figure

However, Fig. (10) represents the change of the s-factor with temperature for the sample contains 15 mol % WO_3 as a representative figure, where it appeared that it decreases with the increase of

temperature. This indicated that, the correlated barrier hopping (CBH) model proposed by Elliot [25] can be used to describe the conductivity mechanism, where the experimental behavior of the exponent factor (s) agree well with those predicted by the model, according to equation (5) [26],

$$s = 1 - \frac{6 k_B T}{W_m + k_B T \ln(\omega \tau_o)} \qquad (5)$$

Where W_m is the barrier height, k_B is Boltzmann constant, T the absolute temperature, is the relaxation time and is the angular frequency.

The obtained conductivity values were plotted as functions of WO_3 content, in Fig. (11) at different fixed temperatures (458,428 and 378 K). It can be seen that by adding tungsten oxide replacing phosphorus oxide up to 15 mol %, the conductivity shows gradual increase, while, when adding more WO_3 the conductivity exhibits sharp decrease (at 458 and 428 K) while at 378 K, the decrease starts at 10 mol % WO_3.

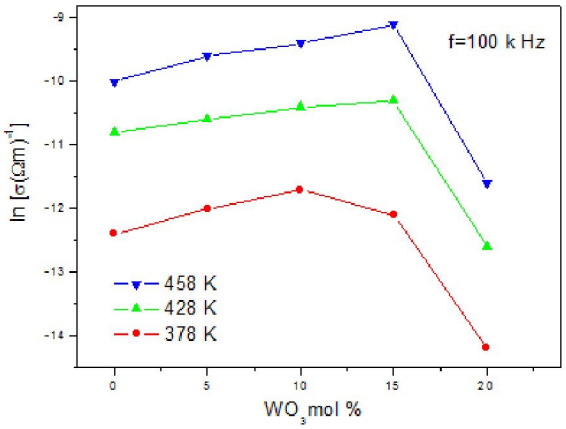

Figure 11. The total conductivity versus WO_3 content, at different fixed temperatures and constant frequency of 100 kHz

It can be supposed that the conductivity in the WO_3 free sample is mainly due to the movement of Na^+ cations. The replacement of P_2O_5 by WO_3 increases the electronic conductivity since tungsten cations occupy five different oxidation states. Hence, the gradual increase of WO_3 increases gradually the total conductivity. The observed sharp decrease of the conductivity after WO_3 reaches 10 mol%, at 378 K and 15 mol% at 428 and 458 K, may be due to:

(i) The blocking effect of the large tungsten cation volume in comparison with the smaller phosphorous cation volume. This was found in agreement with the molar volume and density studies where they showed a gradual decrease in the internal free volume, since some tungsten cations will act to fill the vacancies leading to block the pathways of the charge carriers and hence leads to an effective decrease in the mobility of the present sodium cations.

(ii) The gradual decrease of phosphorous cations may force tungsten cations to occupy some glass former positions, and hence do not participate in the conduction process. This supposition can be confirmed by the appearance of some WO_4 groups in the IR analysis.

The dielectric constant (ε') temperature dependence was studied for the investigated glasses in the temperature range from 300 to 460 K, and at three fixed frequencies (1, 10, 100 kHz.). The observed change in ε' was represented graphically in Fig. (12), for the sample that contains 15 mol% WO_3, as representative figure. It was observed that at low temperatures the dielectric constant is almost independent of temperature and show weak frequency dispersion while at higher temperatures it increases gradually as the temperature was increased, and it shows large frequency dispersion, where it decreases with the increase of frequency.

The reason for these behavior is that, the electric dipoles move almost parallel to the ac external electric field and creates an internal electric field. With the increase of temperature the movement of the electric dipole is easier and then the internal electric field increased which act to increase the dielectric constant values [27].

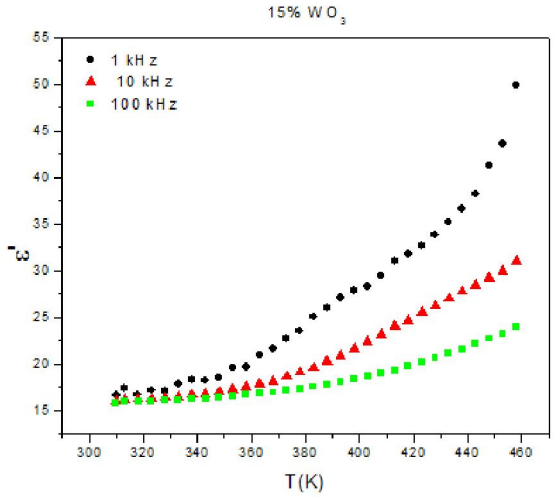

Figure 12. The dielectric constant temperature dependence at different fixed frequencies for the sample that contains 15 mol% WO_3, as representative figure

The dielectric loss factor (ε'') temperature and frequency dependence was also studied. Fig. (13)

exhibits the change in the dielectric loss (ε'') as a function of temperature and frequency for the sample contains 15 mol % WO_3, as representative figure. Similar behaviors were also obtained for all samples.

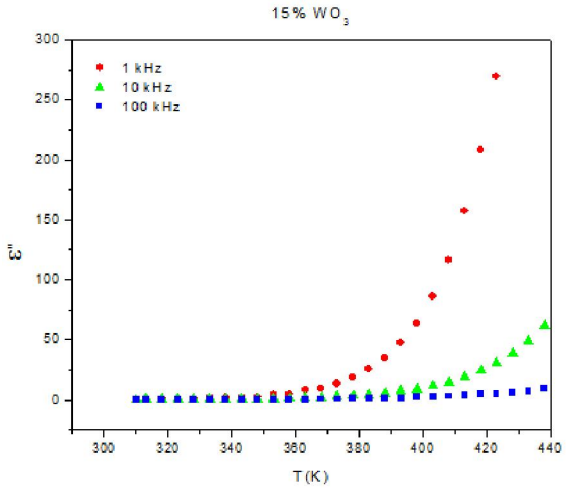

Figure 13. The variation of the dielectric loss versus temperature at different frequencies for the sample containing 15 mol% WO_3, as representative figure

It is noticed that at relatively low temperatures ε'' appeared to be temperature and frequency independent, while at relatively high temperatures, it increases gradually as the temperature was increased such that the rate of increase is inversely proportional to the applied frequency. This behavior can be attributed to the relaxation phenomenon that can be divided into three parts, the conduction loss, the dipolar loss and the vibrational loss. Since the conduction loss is proportional to σ_ω therefore the conduction loss increased as the conductivity increased, (which is a function of temperature), similar behavior was obtained for all other samples. The dielectric loss represents the energy loss from the dielectric and it appeared in many forms (friction between the molecules, radiation …etc.), the friction between the molecules increased by increasing the movement of the dipoles, then the dielectric loss is increased by increasing temperature [28-30].

Figs. (14 and 15) represents the variation of dielectric constant, and dielectric loss respectively as a function of WO_3 content at different fixed temperatures. It can be seen that as WO_3 content was gradually increased, both the dielectric constant and loss show an increase until WO_3 reaches 10 and 15 mol% (for ε' and ε'' respectively) then they start to decrease again. This behavior may be due to the fact that, the dielectric constant (ε') for a dielectric material is directly proportional to the charge (Q) on that material, and inversely proportional to the net electric field value.

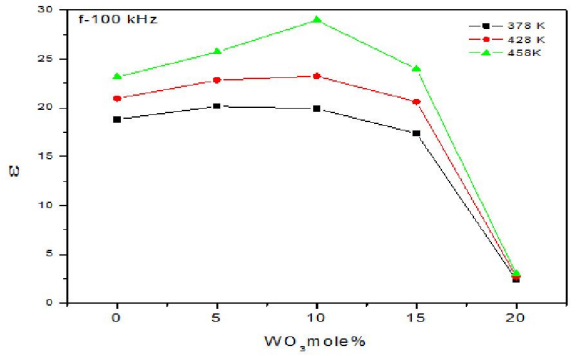

Figure 14. The dielectric constant as a function of WO_3 content at different fixed temperatures

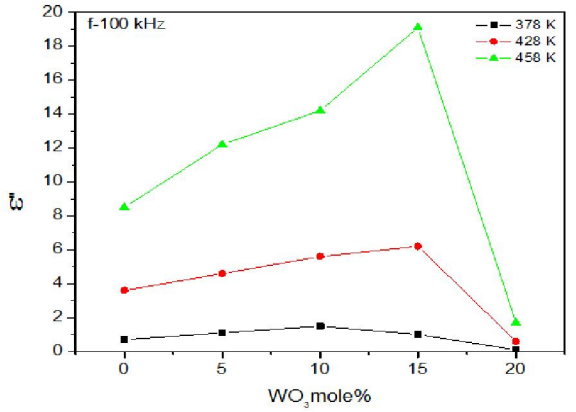

Figure 15. The dielectric loss as a function of WO_3 content at different fixed temperatures

Increasing WO_3 leads to an increase in the conductivity, and then increases the charge (Q) on the material, and then increases the dielectric constant, which act to increase the internal electric field and then decreases the net electric field, which in turn increases the dielectric constant and loss.

After WO_3 reaches 10 and 15 mol % (moderate concentrations of WO_3) a decrease in the conductivity was observed (see Fig. (11)). This leads to decrease the dielectric constant. On the other hand, the decrease of the charge on the material leads to decrease the internal electric field and to increase the net electric field, and hence all these factors act to decrease the dielectric constant and loss.

4. Conclusion

According to the obtained results, within the aim of this work, and as WO_3 (as a heavy metal oxide) was gradually increased; the density showed gradual increase and the molar volume showed gradual decrease. Also, despite of the fluctuations observed in the total conductivity of the studied glasses, all samples showed semi-conduction behavior and the conduction mechanism follows the CBH model. According to the shielding properties

study it can be concluded that gamma-ray shielding glass can be prepared from phosphorus pent-oxide as host glass doped with tungsten oxide. It can be concluded also that, as WO_3 was increased the gamma-ray mass attenuation coefficient increased and consequently the HVL decreased. Finally, all the studied samples can be used as gamma-ray shield for low gamma-ray energies and for radio-active waste encapsulating before interment under-ground. It was concluded also that, the sample that contains 20 mol% WO_3 is the best one for shielding 332 keV gamma-ray energy, since it show the highest μ_t and the lowest HVL values.

Corresponding Author:
Dr. Ahmed G. Mostafa
Physics Department
Faculty of Science, Al-Azhar University, Nasr City, Cairo, Egypt
E-mail: drahmedgamal@yahoo.com

References

1. S. T. Reis, M. Karabulut and D. E. Day, J. Non-Cryst. Solids, 292 (2001) 150.
2. M. Karabulut, E. Metwalli, D. E. Day and R. K. Brow, J. Non-Cryst. Solids, 328 (2003) 199.
3. P. Y. Shih and T. S. Chin, Mater. Chem. And Phys., 60 (1997) 50.
4. A. A. Ramadan, A. G. Mostafa, M. Y. Hassaan, A. Z. Hussein and A. Y. Abdel-Hassib, Isotope and Rad. Res., 46 (1) (2014) 83.
5. M. Srinivasa Reddy, J. Appl., Phys. 37 (2007) 203.
6. S. Fojino and Kuwabara, Key Eng. Mater., 320 (2006) 209.
7. A. Mansingh, R. P. Tandon and J. K. Vaid, Phys. Rev. B, 21 (1980) 4829.
8. B. K. Chaudhary, K. K. Som and A. Ghosh, J. Appl. Phys., 29 (1990) 120.
9. A. Mansingh, V. K. Dhawan and M. Sayer, Philo. Mag. B, 48 (1983) 215.
10. A Mansingh, J K Vaid and R P Tandon, J. Phys. C, 9 (1976) 1809.
11. A. G. Mostafa, M. Y. Hassaan, A. A. Ramadan, A. Z. Hussein and A. Y. Abdel-Hassib, Nature and Science, 11 (5) (2014) 148.
12. A. M. Zoulfakar, M. Sc. Thesis, Al-Azhar Univ. (2013).
13. D. A. Magdas, A, Cosar, V. Chis, I. Ardelean and N. Vedeanu, Vib. Spectrosc., 48 (2008) 251.
14. A. G. Shikerkar, J. A. E. Desa, P. S. R. Krishna and R. Chitra, J. Non-Cryst. Solids, 270 (2000) 234.
15. L. Baia, D. Muresan and M. Baia, Vib. Spectrosc., 43 (2007) 313.
16. S. W. Martin, Eur. J. Solid Inorg. Chem., 28(1) (1991) 163.
17. C. Daynand and M. S. Graw, J. Mater. Sci., 31 (1996) 1945.
18. F. F. Sene, J. R. Martinelli and L. Gomes, J. Non-Cryst. Solids, 348 (2004) 30.
19. J. C. Buyn, B. M. Kim, K. S. Hong, H. J. Jung, S. W. Lee and A. A. Lzyneev, J. Non-Cryst. Solids, 190 (1995) 288.
20. G. B. Rouse, P. J. Miller and W. M. Risen, J. Non-Cryst. Solids, 28 (1978) 193.
21. A. M. Efimov, J. Non-Cryst. Solids, (1997) 209.
22. O. Cazor,D. A. Magdas and I. Ardelean, J. Optoelectronics Advanced Materials, 9 (2007) 1730.
23. U. B. Chanshetti, Phys. Chem. & Technology, 1 (2011) 9.
24. Donna L. Corroll, Ph. D. Thesis, Univ. of Warwick, UK (2008).
25. Elliot, Adv. Phys., 18 (1987) 31.
26. M. S. Aziz, F. Abdel-Wahab, A. G. Mostafa and E. M. El-Agwany, J. Mater. Chim. Phys., 91 (2005) 532.
27. N. F. Mott, J. Non-Cryst. Solids, 1 (1968)1.
28. A. M. Abdel-Ghany, Ph. D. Thesis, Al-Azhar Univ., (2011).
29. Y. M. Moustafa, K. El-Egili, J. Non-Cryst. Solids, 240 (1998) 144.
30. P. Subbalakashmi and N. Veeraiah, J. Non-Cryst. Solids, 298 (2002) 89.

12/20/2014